NANO · MICRO small
www.small-journal.com

A Flexible Loudspeaker Using the Movement of Liquid Metal Induced by Electrochemically Controlled Interfacial Tension

*Sang Woo Jin, Yu Ra Jeong, Heun Park, Kayeon Keum, Geumbee Lee, Yong Hui Lee, Hanchan Lee, Min Su Kim, and Jeong Sook Ha**

A flexible liquid metal loudspeaker (LML) is demonstrated consisting of a gallium-based eutectic liquid metal (Galinstan) and basic aqueous electrolyte ($NaOH_{(aq)}$). The LML is driven by liquid metal motion induced by the electrochemically controlled interfacial tension of the Galinstan in $NaOH_{(aq)}$ electrolyte under an applied alternating current (AC) voltage. The fabricated LML produces sound waves in the human audible frequency band with a sound pressure level of ≈40–50 dB at 1 cm from the device and exhibits mechanical stability under bending deformation with a bending radius of 3 mm. Various sounds can be generated with the LML from a single tone to piano notes and human voices. To understand the underlying mechanism of sound generation by the LML, motion analyses, sound measurements, and electrical characterization are conducted at various frequencies. For the first time, this work suggests a new type of liquid metal-based electrochemically driven sound generator in the field of flexible acoustic devices that can be applied to future wearable electronics.

1. Introduction

With the advent of the fourth industrial revolution, media access without time and space limitations have been realized owing to the wireless Internet.[1] Accordingly, studies on soft portable and wearable acoustic devices have been actively conducted to replace existing heavy and rigid loudspeakers.[2–8] However, due to the lack of diversity in the driving principles, limitations exist in the development of flexible acoustic devices, including difficulties in deformability and the selection of materials and structures. In particular, skin-attachable devices are prone to be strained due to skin movements; therefore, they are required to have mechanical stability under deformations.[3,9–14] Recently, deformable loudspeakers with various sound-producing mechanisms based on dynamic,[2] piezoelectric,[6,15,16] electrostatic,[5] and thermoacoustic[3,7,8] principles have been reported. The loudspeaker based on the dynamic principle is driven by Lorentz forces, which are formed through electromagnetic interaction between the permanent magnet and the current-carrying voice coil.[2,17,18] In piezoelectric principle, vibration is generated by applying electric field to aligned dipoles in the piezoelectric materials.[6,15,16] The electrostatic force generated by the applied high voltage to the stator is also used in the loudspeaker.[5] While those three sound generating methods are all based on electromagnetic interactions, recently reported thermoacoustic devices generate sounds by vibrating surrounding air through thermal expansion and contraction using Joule heat.[3,7,8] Even though such thermoacoustic devices have been actively researched as thin film wearable acoustic devices owing to the application of nanomaterials, the power consumption is relatively high at the level of several watts, and the sound generation is reduced in the low frequency audible band.[5,19,20] Dynamic method has been widely used in commercial acoustic devices, but it was difficult to apply to wearable system because of the use of both rigid magnet and metal voice coil. In our previous work, a stretchable dynamic acoustic device was introduced by replacing a rigid metal voice coil with a liquid metal embedded channel.[2] However, there was still a limit to use rigid NdFeB magnets for sufficiently high sound pressure output. In this study, we introduce a flexible sound source made of gallium-based liquid metal but driven by a magnet-free electrochemical principle.

Gallium-based eutectic liquid metals have been actively studied as next-generation flexible conductors. Among them, Galinstan is a eutectic alloy of Ga (68.5%), In (21.5%), and Sn (10%), which is in a liquid phase at room temperature due to its low freezing point (−19 °C) and has a high electrical conductivity (3.46×10^6 S m^{-1} at 20 °C) while being capable of various deformations.[21–23] Additionally, this material has a low vapor pressure, and the oxide film formed in the air improves its mechanical and electrical stability. Furthermore, Galinstan exhibits a much lower toxicity than mercury, which enables its application to skin-attachable devices.[22,24] Because of these properties, liquid metals have been actively studied as elastic conductors in a variety of soft electronic devices, including simple

S. W. Jin, Dr. G. Lee, M. S. Kim, Prof. J. S. Ha
KU-KIST Graduate School of Converging Science and Technology
Korea University
145 Anam-ro, Seongbuk-gu, Seoul 02841, Republic of Korea
E-mail: jeongsha@korea.ac.kr
Y. R. Jeong, Dr. H. Park, K. Keum, Y. H. Lee, H. Lee, Prof. J. S. Ha
Department of Chemical and Biological Engineering
Korea University
145 Anam-ro, Seongbuk-gu, Seoul 02841, Republic of Korea
The ORCID identification number(s) for the author(s) of this article can be found under https://doi.org/10.1002/smll.201905263.

DOI: 10.1002/smll.201905263

stretchable interconnections,[10,25,26] sensors,[27,28] actuators,[29–33] electrochemical diodes,[34,35] and wireless antennas.[27,36,37] In addition to these various applications, studies on the movement of liquid metal by electrically adjustable interfacial tension in the electrolytes have also been actively conducted.[29–33,38,39] Such a phenomenon can be explained in terms of either electrical double layer formation through the accumulation of charges on the liquid metal surface[29,30,40] or the continuous formation and removal of the oxide film, acting as surfactants.[31,38] In the former method, the motion of the liquid metal is caused by the Marangoni effect from the interfacial tension gradient, while a spread of liquid metal is induced by gravity with a sharp decrease in surface tension due to the surfactant in the latter case.

Most of the studies have been performed with an applied direct current (DC) voltage, while a few reports have shown the alternating current (AC) voltage-induced vibration of Galinstan applied to pumps or stirrers.[29,30] In addition, many studies on liquid metal antennas for generating electromagnetic waves using very high frequency (Megahertz–Gigahertz) AC currents have been reported as shown in Table S1 in the Supporting Information. However, to the best of our knowledge, no study on the loudspeaker generating sound wave in the audible frequency band (20 Hz–20 kHz)[5] was reported using the mechanical vibration of liquid metal.

In this work, we demonstrate a flexible liquid metal loudspeaker (LML) using the electrochemically induced motion of Galinstan in a basic aqueous electrolyte. The LML is driven by the previously reported electrochemically controlled capillarity (ECC) phenomena. While the previous research on ECC focused mainly on the flow motion of liquid metal using DC power, in this study, we note that the sound can be generated through repetitive vibration of liquid metal using AC power. Although the required voltage is below 1 V and the current flowing in the circuit is about several tens of milliampere, the fabricated device produces 40–50 dB of human audible sound when measured at a distance of 1 cm. This is because the ECC phenomenon can change the interfacial tension of the liquid metal with low power consumption. This work can lead to the development of device interacting acoustically with humans, unlike wireless antennas that can be applied to wireless powering of the active devices or data transmission. The developed LML consists of two Galinstan-wetted copper (Cu) foil electrodes on a flexible substrate in sodium hydroxide aqueous ($NaOH_{(aq)}$) electrolyte. An elastic polymer reservoir made of Ecoflex is used to prevent leakage of the liquid electrolyte. With a variation in the concentration of the NaOH solution, applied bias voltage, and volume of Galinstan, the acoustic performance is investigated to understand the sound generation mechanism. Our LML exhibits mechanical stability under bending deformation with a bending radius of 3 mm and reproduces the sound signal from a single tone, piano notes, and human voices. This is the first demonstration of a flexible loudspeaker based on sound generation by the electrochemically induced motion of the liquid metal Galinstan.

2. Results and Discussion

As shown in **Figure 1**a, the flexible LML consists of two Galinstan-wetted Cu foil electrodes and a 1 M $NaOH_{(aq)}$ electrolyte on a flexible substrate. Here, the copper foil electrode was used to hold the liquid metal in an oxide-free environment. The structure is basically the same as that of an electrochemical capacitor. The developed device produces sound waves via electrochemically induced motions of the Galinstan.[31,32,38,39] Figure 1b illustrates the movement of Galinstan by the electrochemically controlled interfacial tension in the fabricated LML and the generation of vibration when the AC signal is applied. According to the polarity change of the electrode due to use of AC input bias, the movement of the Galinstan can be schematically explained in Figure S1 in the Supporting Information. As clearly demonstrated, repetitive oxidation–reduction induced movement of the Galinstan drop can generate a sound by vibrating surrounding medium. Briefly, when oxidative potential is applied to Galinstan, a thin oxide layer (Ga_2O_3) is formed on the surface by the following reaction[31,41]

$$2Ga + 3H_2O \rightarrow Ga_2O_3 + 6H^+ + 6e^- \quad (1)$$

The shape of the liquid metal is formed when the interfacial tension and gravity are in balance.[32,38] Upon formation of gallium oxide, the interfacial tension is reduced to induce the spreading of liquid metal by gravity since the gallium oxide acts as a surfactant. In addition to the gravity, interfacial tension gradients due to nonuniform distribution of oxide can also influence on the shape since oxidation is more active on the Galinstan surface close to the counter electrode. Such gradient of the interfacial tension might cause a pressure differential inside the Galinstan cap, inducing the flow of the liquid metal toward the counter electrode.[29] However, when the reductive potential is subsequently applied, the oxide film can be reduced, which causes the Galinstan to retract instead of spreading. This process is continuously repeated under an AC bias, causing the liquid metal to vibrate. In this iterative process, the lifetime of the device limited by the dissolution of gallium in the electrolyte was calculated by measuring the mass loss with operation time, as described in Figure S2 in the Supporting Information. A more detailed description of the working principle of the LML is given in Figure 3a. Figure 1c shows the optical images taken from the LML with the Galinstan/1 M $NaOH_{(aq)}$/Galinstan system before and after the application of the AC signal. Here, Cu electrodes (2.5 cm × 0.3 cm) were wetted with 80 µL of Galinstan.

In all the figures related with the measurements in Galinstan/$NaOH_{(aq)}$/Pt, the potential is noted as an effective potential value of V_{net} (= V_{in} − $V_{galvanic}$), excluding the potential $V_{galvanic}$ (≈1.4 V) due to the galvanic cell effect between Pt and Galinstan from the input potential (V_{in}). Therefore, in the case of the open-circuit potential (V_{net} = 0 V), the input voltage (V_{in}) applied to the circuit is 1.4 V. The interfacial tension of the Galinstan droplet according to the applied redox DC potential was measured by the sessile drop method, as shown in Figure 1d.[38,42] The interfacial tension decreased with increasing oxidative and reductive potentials. The largest interfacial tension value of ≈500 mJ cm^{-2} was measured at a potential of zero charge (V_{net} = 0 V), consistent with the previously reported results.[38] Symmetrical Galinstan/Cu electrodes were used to fabricate the LML without such an undesired galvanic effect. In those cases, V_{net} is equal to V_{in} because $V_{galvanic}$ is zero in all acoustic

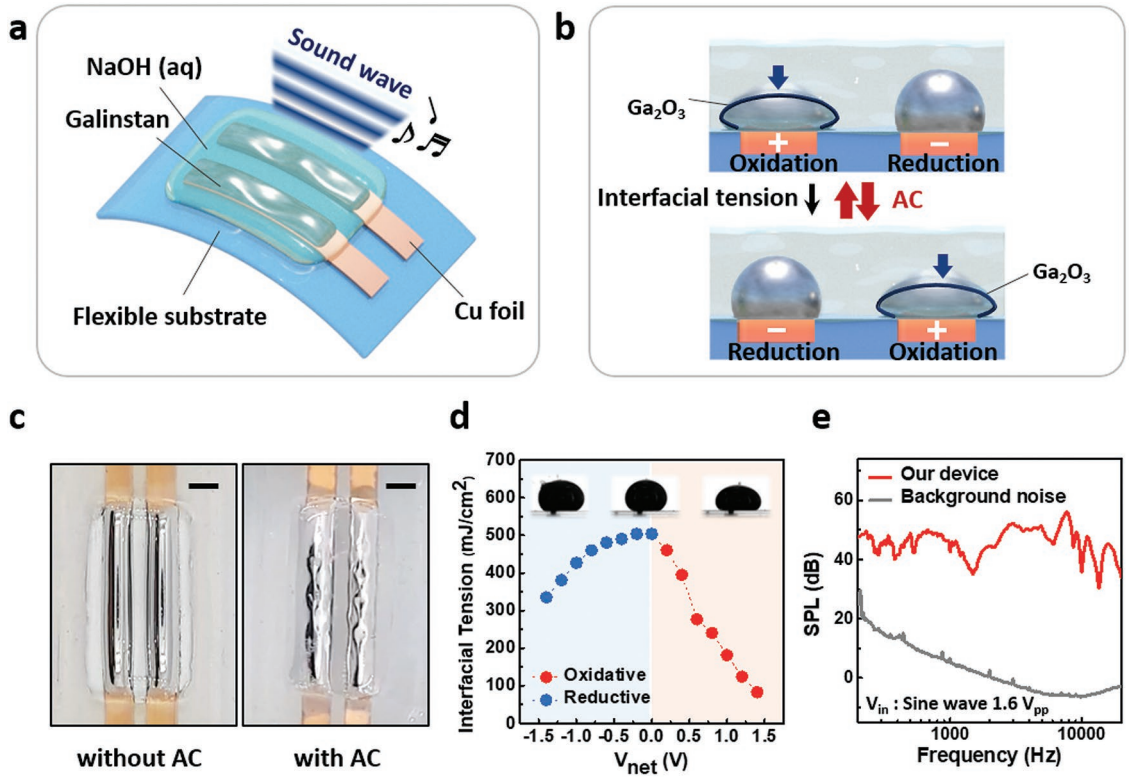

Figure 1. a) Schematic illustration of the fabricated LML. b) Schematic illustration of the movement of Galinstan under applied oxidation and reduction potentials, respectively. Here, the blue arrows indicate the flowing direction of Galinstan under applied oxidative and reductive potentials, respectively. c) Optical images of the LML without (left) and with (right) applied AC voltage. (scale bar: 0.3 cm) d) Measured interfacial tension of the Galinstan droplet according to the applied DC bias (V_{net}). The inset images show the appearance of the Galinstan droplet according to the applied potential of $V_{net} = -1.5$, 0, and 1.5 V, respectively. e) Frequency response curve (SPL vs f) of the LML.

measurements. A sinusoidal signal (1.6 V_{pp}) of the audible frequency band (200 Hz–20 kHz) was applied to the LML to induce the vibration of Galinstan, and a sound pressure level (SPL) of 40–50 dB was measured at a distance of 1 cm from the device, as shown in Figure 1e. This SPL (dB) corresponds to about 2–6 mPa in pressure units by the Equation (2) below[43]

$$\tilde{p} = p_0 \times 10^{\frac{L_p}{20}} \quad (2)$$

where, p_0 is a reference sound pressure (20 µPa), $\tilde{p}$ is a pressure (Pa), and L_p is a sound pressure level (dB). Here, 1 M $NaOH_{(aq)}$ was used as an electrolyte. Video S1 in the Supporting Information shows that the fabricated LML can produce a human-perceptible level of sound. Further analyses were conducted to understand the detailed driving principles and characteristics of the developed LML.

To investigate the acoustic performance of the LML under various conditions, SPLs were measured according to the $NaOH_{(aq)}$ concentrations, amplitudes (V_{in}), and frequencies (f) of the input signals. The shape of V_{in} was fixed with a sine wave. First, as the V_{in} increased, the SPL generally tended to increase in **Figure 2**. Figure S3a in the Supporting Information shows that at higher input voltages, the redox current increased. As the redox current increased, the redox reaction rate of Galinstan became faster, and consequently, the motion of the Galinstan became faster.[31] Therefore, when the concentration of $NaOH_{(aq)}$ increased from 0.1 to 1.0 M, the SPL at the same input voltages was increased accordingly. This finding is due to the decrease of impedance with the increase of the electrolyte concentration (Figure S4, Supporting Information), which leads to an increase in the redox current. Impedance and SPL of the fabricated LML with high concentration NaOH electrolyte (>1 M) were also investigated. As shown in Figures S4 and S5 in the Supporting Information, increase of the concentration up to 3 M resulted in the decrease of impedance but the increase of SPL. The increase of SPL is attributed to the increase in the redox current as a result of the decreased impedance. With further increase to 6 M, there was no significant difference in impedance compared to use of 3 M. Accordingly, no noticeable enhancement in the SPL was observed above 3 M regardless of the frequency. In addition, it was also confirmed that the impedance of the LML was lower at higher frequencies due to its capacitor characteristics, as shown in Figure S4 in the Supporting Information.[44]

Although the SPL caused by liquid metal vibration depends on voltage and current, it is also affected by various factors such as the vibration characteristics of the liquid metal, electrolyte, and surrounding elastomer. The effect of these vibration characteristics is expected to be a major factor in showing the nonlinear response, especially in the low frequency band under 1 kHz. Optimizations for the response to low frequencies

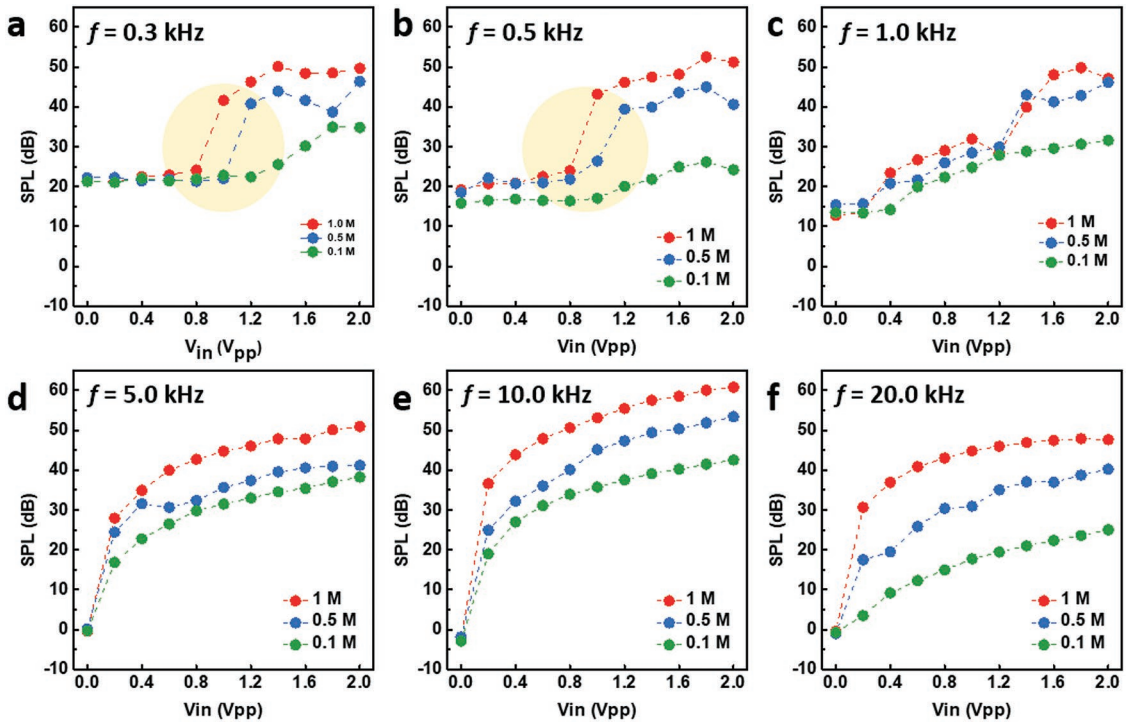

Figure 2. Acoustic performance according to the input voltage amplitudes (V_{in}) and electrolyte concentrations at a specific frequency of a) 0.3 kHz, b) 0.5 kHz, c) 1.0 kHz, d) 5.0 kHz, e) 10 kHz, and f) 20 kHz, respectively.

would require careful tuning process through computer simulation and acoustical analysis. Interestingly, a threshold voltage was observed at low frequencies below 1 kHz. Figure 2a,b shows that the sound pressure was suddenly formed at an input voltage between 0.8 and 1.2 V_{pp} at frequencies of 300 and 500 Hz, marked as yellow circles. It was shown that the SPL was higher than the background (BG) noise by ≈20–30 dB above those threshold voltages, but it was not distinguishable from the BG noise below the threshold voltages. This discontinuity was neither sufficiently understood by the ohmic relationship between the voltage and the current nor by the impedance analysis. To understand this phenomenon, further investigation was performed in the following parts.

To understand the motion of Galinstan under an applied AC bias voltage, it is a prerequisite to understand the movement of Galinstan under a DC bias voltage. As schematically illustrated in **Figure 3**a, when Galinstan is in the potential of zero charge (PZC) state and the oxide layer of Galinstan is removed by $NaOH_{(aq)}$ electrolyte, it has the largest interfacial tension.[38] If a reductive potential is applied to the Galinstan, then positive ions are adsorbed on the surface to form an electrical double layer (EDL). This capacitive charging reduces the interfacial tension (γ) of the Galinstan, i.e., electrocapillarity (EC) and it can be expressed by the following Lippman's Equation (3).[29,32,39,40]

$$\gamma(V) = \gamma_0 - \frac{C}{2}V^2 \tag{3}$$

where γ_0 is the interfacial tension at the PZC, C is the capacitance at the electrical double layer, and V refers to electrical potential across the EDL with $V = V_{in} - V_{PZC}$ in this work. In contrast, when an oxidative potential is applied to Galinstan, a gallium oxide layer is formed on the surface. These oxides act as surfactants and reduce the interfacial tension of Galinstan.[31,38,45] Previous studies have shown that continuous electrochemical oxidation and etching can induce the flow of Galinstan, and this phenomenon is referred to as ECC.[31,38,45]

To understand the motion of the Galinstan according to the applied AC signal amplitudes and frequencies in detail, real-time current measurement and Galinstan motion analyses were performed, as shown in Figure 3b,c. The motion of the Galinstan to the applied effective potential (V_{net}) was recorded in real time using a charge-coupled device (CCD) camera and potentiostat equipment, as shown in Figure 3a. To clearly see the change in the current and the movement of the Galinstan according to the effective voltages (V_{net}), square waves with a constant voltage of 1.2 V were applied. The change in the current and the shape of Galinstan at the corresponding time were measured when the net oxidative pulse of 1.2 V was applied to the Galinstan, as shown in Figure 3b,c. Each pulse was applied for 10 and 2.5 s, corresponding to 0.05 and 2 Hz, respectively. During the remainder of the interval, an open-circuit voltage (V_{net} = 0 V) was applied. Current curves consisting of a peak and plateau were obtained from the current measurement over time. The formation of the peak and the rapid decline of current are mainly attributed to the formation of gallium oxide and capacitive charging. When the gallium oxide thickens or the electrode is fully charged, a plateau state with low current is maintained.[34,46] Interestingly, the rapid movement of liquid metal occurred at very short time intervals near the current peak between t_1 and t_2 in Figure 3b,c. At the current plateau during the remainder of the interval between t_2 and t_3,

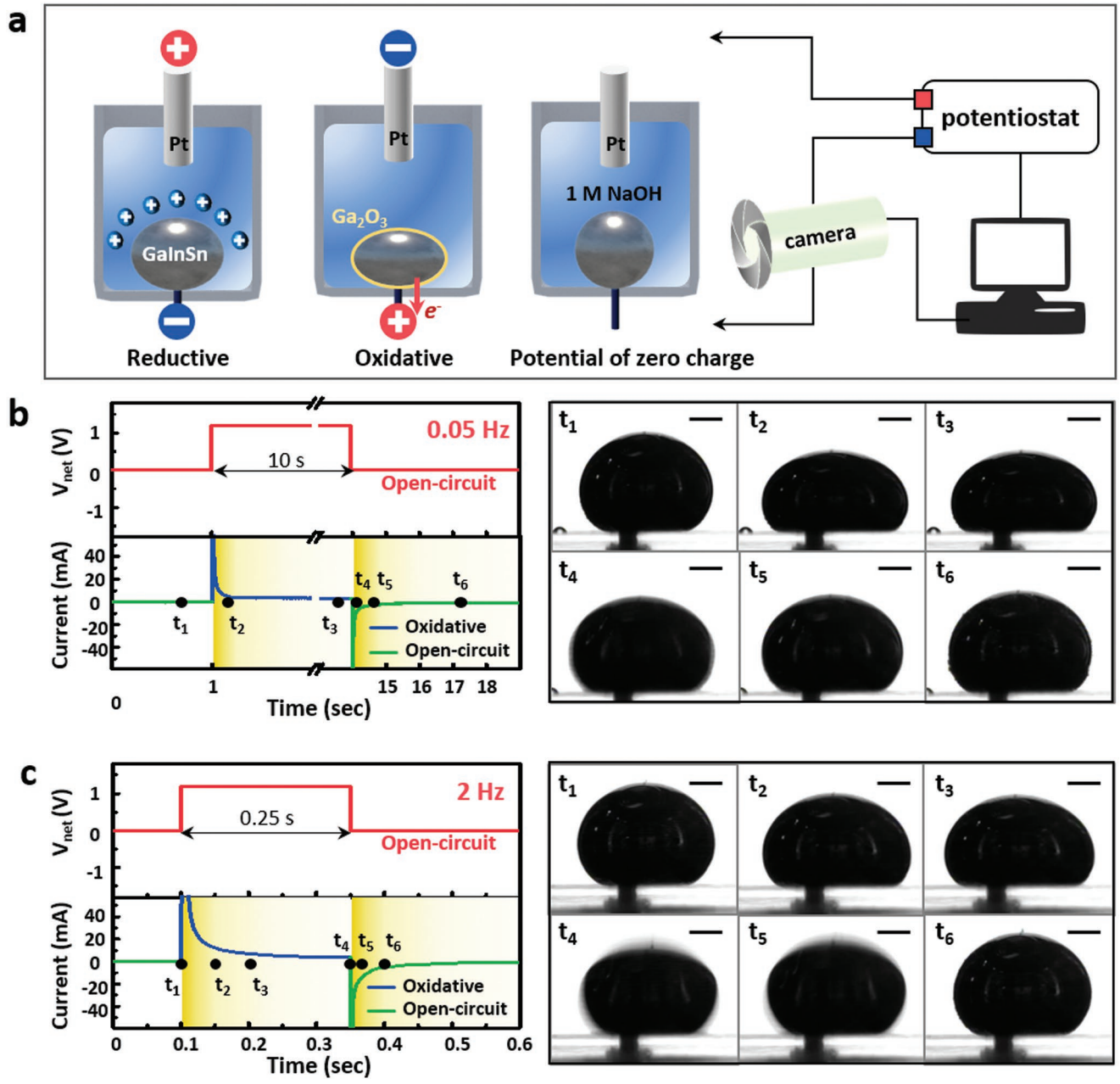

Figure 3. a) Schematic illustration of the working principle of the LML under applied DC bias voltages. Analysis of Galinstan motion with an applied square-shaped oxidative pulse for b) 10 s (equivalent to 0.05 Hz) and c) 0.25 s (equivalent to 2 Hz), with the corresponding images of Galinstan droplets (scale bar: 1.1 mm).

the liquid metal showed a very slow motion or suspended state, even though the oxidative potential was still applied. In addition, as the oxidative potential disappeared at t_4, the grown oxide layer was rapidly reduced away by $NaOH_{(aq)}$ so that the liquid metal quickly returned to its original shape. During the time between t_5 and t_6 in Figure 3b, when the current hardly flowed, the movement of the Galinstan was negligible. In summary, at the moment when an oxidative potential began to be applied to the Galinstan (between t_1 and t_2), the formation of oxide at the surface causes the rapid movement of the liquid metal.[31,38] After the decrease of the current due to the increase of oxide thickness, the motion of a Galinstan droplet induced by the change of the interfacial tension reached equilibrium at the point between t_2 and t_3.[34] In addition, when the open-circuit potential was applied right after the pulse at t_4, the reverse current was observed. This reversal might be attributed to the reduction in the oxide layer by $NaOH_{(aq)}$ or the discharge of the ions attached on the surface of the electrodes.

As shown in Figure 3c, the lowering of the interfacial tension due to the formation of oxide film occurs in a very short time of about 0.05 s at a current peak between t_1 and t_2. On the other hand, after removal of the applied oxidation bias voltage

to liquid metal, the process of returning the liquid metal droplet to its original shape occurs in a time about 0.5 s between t_4 and t_6 in Figure 3c. Such a time difference can be related to the rate at which the previously formed oxide film is dissolved by the NaOH electrolyte. Therefore, it can be expected that the electrical oxidation of liquid metal occurs about an order of magnitude faster than the natural dissolution of oxide by $NaOH_{(aq)}$.

Measurements similar to those in Figure 3c were conducted under a full cycle of AC pulse in Figure S6 in the Supporting Information. Contrary to our initial expectation that the liquid metal would pass through the highest interfacial tension state at $V = V_{PZC,}$ where the oxidation voltage was changed to the reduction voltage, liquid metals were converted rapidly from ECC to EC without passing the PZC state. This is probably due to the simultaneous removal of gallium oxide and the formation of the electrical double layer on the droplet surface by accumulation of cations.

It is worth mentioning that even at the reduction potential, a current-time curve consisting of a peak and plateau, similar to that under oxidative potential conditions, was obtained, as shown in Figure S7 in the Supporting Information. However, since the oxide film was not formed under the reductive potential, this phenomenon was purely due to ion charging on the electrode surface. Thus, the reverse current generated at the applied open-circuit voltage immediately after the application of the oxidative pulse was higher than that of the reductive case, indicating the formation of gallium oxide even under a very short oxidation pulse.[34] Despite the fast oxidation rates, however, liquid metal is not expected to reach its final shape under AC voltages with high frequencies but return to its original spherical shape (PZC shape), unlike the case under applied DC voltage in Figure 1d. If the liquid metal formed its equilibrium shape, the redox current would be saturated. However, the measured redox current was not saturated until the half cycle ended at high frequencies and high applied voltages as observed in Figure S3 in the Supporting Information. In addition, these time-dependent current measurements in Figure S3 in the Supporting Information could be a clue to understanding the threshold voltage at the low frequencies of 0.3 and 0.5 kHz observed in Figure 2a,b. As shown in Figure S3b in the Supporting Information, as the period of the pulse became shorter at higher frequencies, the magnitude of current reduction became smaller. This behavior means that the oscillation period of the Galinstan is close to the period of the input signal as the frequency and amplitude of the input signal increase. Moreover, at higher input voltages at the same frequency, not only were the overall current levels increased, but the current decay to plateau was reduced, as shown in Figure S3b in the Supporting Information. As shown in Figure S8 in the Supporting Information, such a phenomenon was rarely observed in the $Pt/NaOH_{(aq)}/Pt$ system, indicating that a slow current decay at high voltage in the Galinstan/$NaOH_{(aq)}$/Pt system was associated with the oxidation and the resultant motion of the Galinstan droplet. The higher the voltage is, the larger the surface expansion (Galinstan motion) is.[38] During this period of motion, electrochemical oxidation and chemical etching occur consecutively, resulting in the slow current decay due to the thickening of gallium oxide layers.[34] From these results, it can be expected that the higher the frequency and the higher the input voltage are, the closer the motion of the Galinstan becomes to the input signal period. For the same reason, when the input voltage was not large enough at low frequencies, it can be deduced that the threshold voltage was formed because the input signal period could not be satisfied, and the amplitude of the droplet vibration was not sufficient. After further studies with high frame rate and resolution-based motion analysis in the future, we expect to provide a better understanding of the working principles.

To investigate the effect of the Galinstan volume on the acoustic performance, the SPL and impedance were measured. **Figure 4**a shows the measured SPL with a variation in the volume of wetted Galinstan on the same sized Cu foil (2.5 cm × 0.3 cm, channel gap: 2 mm). To investigate the contribution of the thermoacoustic effect to the acoustic performance of the fabricated LML, a device using only Cu foil without Galinstan was fabricated. SPLs of 10 and 30 dB were generated at frequencies of 5 kHz and 10–20 kHz, respectively, compared to the BG noise. At frequencies below 1 kHz, the signal could not be distinguished from the BG noise. This finding agreed with the thermoacoustic effect, which was favorable to sound generation at higher frequencies. Compared to the surface-wetted electrode (<5 µL electrode), the SPL increases by 10–40 dB at frequencies above 5 kHz. Considering that the impedance difference between the Cu electrode and the slightly wetted electrode (<5 µL electrode) was very small and that the decibel unit is a log scale, the main sound source was

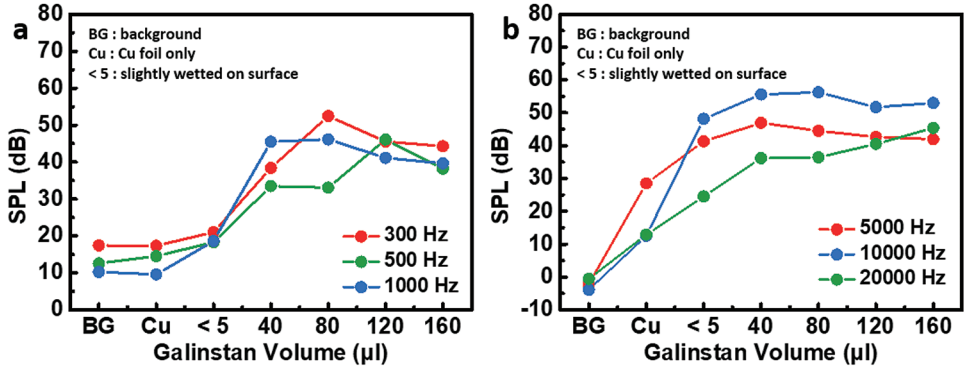

Figure 4. a) Measured SPL according to the Galinstan volume with a variation in the frequency from 300 Hz to 1 kHz. b) Measured SPL according to the Galinstan volume in the frequencies between 5 and 20 kHz.

the vibration caused by the redox reaction of the Galinstan, as shown in Figure 4 and Figure S9 in the Supporting Information.

It was observed that the volume of Galinstan required for generating high SPLs was different depending on the frequency of the AC input signal. At frequencies above 5 kHz, a larger sound pressure of ≈10–40 dB compared to the BG noise was formed, even with the <5 μL electrode; however, it was hardly formed at frequencies below 1 kHz, as shown in Figure 4a,b. This result seems to suggest that the shape change of liquid metal be rarely caused with a small sized liquid metal.[47] In addition, due to the characteristics of a low-frequency vibration with long wavelength, it is expected that the vibration cannot be smoothly performed under a certain volume of Galinstan.[48]

The effect of the gap distance between the two electrodes on the device performance was also investigated. As shown in Figure S10a,b in the Supporting Information, the impedance of the device increased with the increase of the gap distance. Accordingly, the performance of the acoustic device was expected to degrade with the reduction of redox current. As shown in Figure S10c,d in the Supporting Information, compared to the SPL of 6 mm gap distance, that of 2 mm gap is noticeably higher over the whole range of frequency, consistent with the lower impedance. However, the change of SPL at certain frequencies with increase of gap distance to 4 mm was not consistent with the gap distance dependent behavior of impedance. This is probably due to the change in vibration characteristics of the device due to the change in the device structure. Next, we investigated the mechanical stability of the fabricated LML under bending deformation. **Figure 5**a,b and Video S2 in the Supporting Information show that the sound was stably generated regardless of the bending deformation up to the bending radius of 3 mm. In Figure 5b, SPL changed slightly with respect to the bending, probably due to the change in the vibration characteristics by the change in the shape and stiffness of the driving part and surrounding polymer reservoir.[49,50] The fabricated LML played not only single-tone signals but also piano sounds and human voices, as demonstrated in Figure 5c,d and Video S3 in the Supporting Information. As shown in Figure 5c,d, the waveforms of the input signal and the output sound wave were very similar. Slight differences between the input and output waveforms were attributed to the ambient noise filtering process from the extracted audio signals as well as the distortion caused by the frequency response of the device.

Of particular interest, the sound was observed to be much larger and clearer when the microphone directly touched the surface of the device, as shown in Video S4 in the Supporting Information. To verify this phenomenon, the frequency response of the LML was measured in two different cases, as shown in Figure 5e, namely the microphone is apart from the LML through a 1 cm air gap and contacts the LML through the poly(dimethylsiloxane) (PDMS) gap. Here, a 1 cm thick PDMS block was inserted between the microphone and the LML to keep the distance between the microphone and LML constant. It was confirmed that when the microphone directly contacted the PDMS gap, there was a sound enhancement of ≈20 dB at frequencies below 3 kHz, as shown Figure 5f. Video S4 in the Supporting Information also shows that the encapsulation enhances the acoustic performance of the LML with clearer sound, attributed to the reduction of distortion and noise caused by the vibration of liquid phase electrolyte.[51,52] Thus, it indicates that the reservoir and the liquid electrolyte surrounding the Galinstan electrode did not work as proper diaphragms for the efficient conversion of the vibration of Galinstan to sound. Instead of absorbing materials such as PDMS and Ecoflex, use of other flexible polymers with smaller thickness and higher modulus as a diaphragm might be better for acoustic performance. However, PDMS and Ecoflex show the advantage of high mechanical stability over the deformation. As shown in Figure S11 in the Supporting Information, it was confirmed that the elastic Ecoflex reservoir could withstand a vertical pressure of 140 kPa under deformation. However, bending with a bending radius smaller than 2 mm caused the leakage of the electrolyte through the gap between the Cu foil and the Ecoflex, since there appeared exfoliation of the Cu foil from the surrounding polymer due to the induced high pressure of electrolyte by the excessive deformation of the device. These problems might be solved by using a gel electrolyte instead of a liquid electrolyte. It is also necessary to search for safe electrolytes that can replace the currently used strong base electrolytes ($NaOH_{(aq)}$). In addition to the liquid electrolyte issues, there was a problem associated with bubble formation to be addressed for practical applications, which was reported in previous studies.[31] Keeping the AC signal lower than the water electrolysis voltage slows down the formation of bubbles, but they slowly accumulated when the LML was encapsulated, as shown in Figure S12 in the Supporting Information.

Problems associated with the fixation of Galinstan in an oxide-free environment should also be addressed. In the present LML configuration, when the LML was tilted or bent, a flow of liquid metal was observed as shown in Figure S12 in the Supporting Information, which can change the acoustic properties. Also, the tilting or bending can cause the separation of Galinstan from the Cu foil when the Galinstan volume exceeds a certain critical level. This problem is likely to be improved through the structural modification of Cu electrode or use of gel electrolytes. It would be also interesting to control the viscosity of liquid metals to prevent the separation of Galinstan from the Cu foil and to adjust the vibration characteristics of the device. Various studies have been conducted to change the properties of liquid metal by alloying metal nanoparticles to the liquid metal.[22] Depending on the type of nanoparticles to add, the magnetic properties or freezing point of the liquid metal can be adjusted. In particular, addition of Cu nanoparticles can increase the viscosity of liquid metal via electrochemical amalgamation. Since vibration characteristics are affected by the viscosity or modulus of the material,[2] the frequency response of the speaker with respect to the addition of nanoparticles can be studied in future research. Considering these results, further research is needed with respect to the materials and structure as well as on the driving principle for more practical flexible LMLs.

Based on the measurements conducted in this work, we can get relationships between the SPL and the experimental parameters as follows: $SPL \propto I \propto V$, Z^{-1}, C_{NaOH}, d^{-1}, where I is the redox current, V is the amplitude of the applied voltage, Z is the impedance of the fabricated device, C_{NaOH} is the concentration of electrolyte, and d is the gap distance between two electrodes, respectively. At this moment, it is not possible to suggest an analytical equation to explain the influence of the experimental

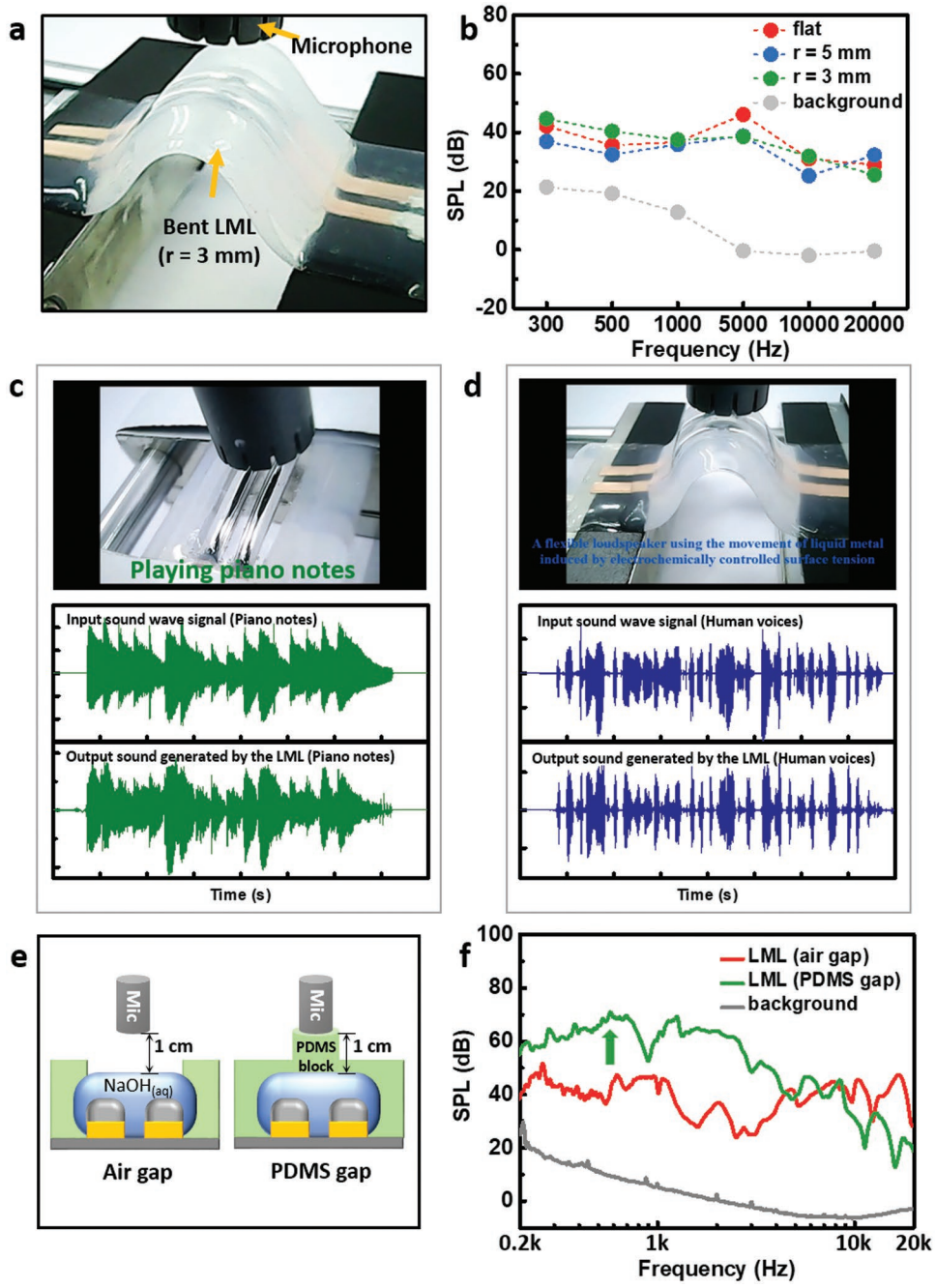

Figure 5. a) A liquid metal loudspeaker (LML) that generates sound in a bent state (an image from Video S2 in the Supporting Information). b) Frequency response (*f* vs SPL) according to the bending radius (*r*) of the device. Snapshots extracted from the Video S3 in the Supporting Information and corresponding input wave signal and output sound wave generated by the LML. c) Piano notes and d) human voices. e) Experimental setup to analyze frequency response in direct contact with microphone. f) Frequency response (*f* vs SPL) according to experimental setup in (e).

parameters on the device performance, for an example, SPL, more quantitatively. However, we expect that in future research, measurement of instantaneous velocity of vibrating liquid metals using high speed microscopes or development of appropriate physical models through computer simulations can predict the device performance better. Perhaps it is also a good approach to directly measure the force or pressure generated by ECC phenomena using a very sensitive force gauge.

3. Conclusion

We have shown that the sound generation by the electrochemically induced motion of liquid metal can be used as the driving principle of a flexible acoustic device. It is confirmed that our LML with a structure of an electrochemical capacitor composed of two liquid metal electrodes and a basic aqueous electrolyte generates sound successfully when an AC signal of the auditory

frequency band is applied. The measured frequency response of the LML and the recorded videos confirm that the LML works well even when it is bent. In addition, systematic studies on the various parameters influencing the SPL of the LML provide an understanding of the sound generation mechanism to develop practical flexible acoustic devices. This work demonstrates a new way of facilely fabricating flexible loudspeakers that can be applied to future wearable electronics.

4. Experimental Section

Fabrication of a Flexible LML: The LML was fabricated by attaching two Cu foils or Cu tapes to a flexible substrate (polyethylene terephthalate (PET) film) with a constant channel spacing (0.2 cm) and wetting Galinstan on a Cu electrode in 1 M NaOH aqueous electrolytes.[27] Specifically, when the Cu foil was attached, uncured Ecoflex (smooth on, Ecoflex 0030) was used as an adhesive. The thickness of the Cu foil was 20 μm. To prevent leakage of the electrolyte, a reservoir made of Ecoflex was fabricated. This process was carried out by first fabricating the reservoir-structured Ecoflex film and then pasting it on the preformed electrodes using uncured Ecoflex as an adhesive. Ecoflex was cured by heating in a 65 °C oven for 30 min using a mixture of the main and curing agent with a mass ratio of 5:5.

Measurement of Acoustic Performance of the Fabricated LML: A desktop-based measuring system consisting of REW (Room EQ Wizard) software and a microphone (Umik-1, miniDSP) was used to measure the SPL. Measurements were carried out in a custom-made noise-proof box for BG noise reduction. All the SPLs were measured with a microphone placed 1 cm apart from the LML. The input AC signal was applied using a function generator (AFG-2125, GwInstek), and an oscilloscope (GDS-1072A-7, GwInstek) was used to find the exact voltage applied to the device.

Measurement of Electrical Properties and Interfacial Tension of Galinstan: Electrical measurements were carried out using a potentiostat instrument. Since the redox reaction can simultaneously occur at both electrodes with the device configuration of Galinstan/NaOH(aq)/Galinstan as shown in Figure S13a in the Supporting Information, it was difficult to observe the actual behavior of a Galinstan droplet. Thus, all the measurements were done in the Pt/NaOH(aq)/Galinstan system as shown in Figure S13b in the Supporting Information. When the measurement was performed in the Pt/$NaOH_{(aq)}$/Galinstan system, an opposite voltage was applied to cancel the induced voltage due to the galvanic cell effect. Unless otherwise noted, all impedance and current measurements were carried out with an electrode of 2.5 cm × 0.3 cm with 80 μL of wetted Galinstan and a Pt counter electrode positioned at a channel spacing of 0.2 cm. During the measurements on impedance, the shape of the electrode and that of Galinstan were kept constant. The amplitude of the voltage for measuring impedance was set to 10 mV. For the measurement of interfacial tension and motion analysis, an enamel Cu wire was connected to the bottom of 40 μL of a Galinstan droplet, and a Pt counter electrode was placed at a height of ≈0.2 cm from the top of the Galinstan droplet. The input signal was supplied using the potentiostat equipment, and droplet motion was recorded in real time using a CCD camera of the contact angle equipment (phx300, SEO).

Supporting Information

Supporting Information is available from the Wiley Online Library or from the author.

Acknowledgements

This work was supported by a National Research Foundation of Korea (NRF) grant funded by the Korean government (MSIP) (Grant No. NRF-2019R1A2B5B03069545). The authors also thank the KU-KIST graduate school program of Korea University.

Conflict of Interest

The authors declare no conflict of interest.

Keywords

acoustic device, electrochemical wetting, flexible loudspeaker, interfacial tension, liquid metal

Received: September 16, 2019
Revised: October 22, 2019
Published online:

[1] M. Hermann, T. Pentek, B. Otto, presented at *Proc. 49th Hawaii Int. Conf. on Syst. Sciences* HICSS, Hawaii, USA, January **2016**.
[2] S. W. Jin, J. Park, S. Y. Hong, H. Park, Y. R. Jeong, J. Park, S.-S. Lee, J. S. Ha, *Sci. Rep.* **2015**, *5*, 11695.
[3] S. Kang, S. Cho, R. Shanker, H. Lee, J. Park, D.-S. Um, Y. Lee, H. Ko, *Sci. Adv.* **2018**, *4*, eaas8772.
[4] C. Keplinger, J. Y. Sun, C. C. Foo, P. Rothemund, G. M. Whitesides, Z. Suo, *Science* **2013**, *341*, 984.
[5] Q. Zhou, A. Zettl, *Appl. Phys. Lett.* **2013**, *102*, 223109.
[6] S. C. Xu, B. Y. Man, S. Z. Jiang, C. S. Chen, C. Yang, M. Liu, X. G. Gao, Z. C. Sun, C. Zhang, *Appl. Phys. Lett.* **2013**, *102*, 151902.
[7] L. Xiao, Z. Chen, C. Feng, L. Liu, Z.-Q. Bai, Y. Wang, L. Qian, Y. Zhang, Q. Li, K. Jiang, S. Fan, *Nano Lett.* **2008**, *8*, 4539.
[8] J. W. Suk, K. Kirk, Y. F. Hao, N. A. Hall, R. S. Ruoff, *Adv. Mater.* **2012**, *24*, 6342.
[9] D.-H. Kim, R. Ghaffari, N. Lu, J. A. Rogers, *Annu. Rev. Biomed. Eng.* **2012**, *14*, 113.
[10] Y. R. Jeong, G. Lee, H. Park, J. S. Ha, *Acc. Chem. Res.* **2019**, *52*, 91.
[11] Y. Liu, M. Pharr, G. A. Salvatore, *ACS Nano* **2017**, *11*, 9614.
[12] A. Choe, J. Yeom, R. Shanker, M. P. Kim, S. Kang, H. Ko, *NPG Asia Mater.* **2018**, *10*, 912.
[13] C. Choi, Y. Lee, K. W. Cho, J. H. Koo, D.-H. Kim, *Acc. Chem. Res.* **2019**, *52*, 73.
[14] T. R. Ray, J. Choi, A. J. Bandodkar, S. Krishnan, P. Gutruf, L. Tian, R. Ghaffari, J. A. Rogers, *Chem. Rev.* **2019**, *119*, 5461.
[15] T. Sugimoto, K. Ono, A. Ando, K. Kurozumi, A. Hara, Y. Morita, A. Miura, *Appl. Acoust.* **2009**, *70*, 1021.
[16] S. Xu, B. Man, S. Jiang, M. Liu, C. Yang, C. Chen, C. Zhang, *CrystEngComm* **2014**, *16*, 3532.
[17] G. Y. Hwang, K. T. Kim, S. U. Chung, S. M. Hwang, B. S. Kang, I. C. Hwang, *J. Appl. Phys.* **2002**, *91*, 6979.
[18] E. W. Siemens, *US 149797*, **1874**.
[19] H. Tian, T.-L. Ren, D. Xie, Y.-F. Wang, C.-J. Zhou, T.-T. Feng, D. Fu, Y. Yang, P.-G. Peng, L.-G. Wang, L.-T. Liu, *ACS Nano* **2011**, *5*, 4878.
[20] H. Tian, D. Xie, Y. Yang, T.-L. Ren, Y.-F. Wang, C.-J. Zhou, P.-G. Peng, L.-G. Wang, L.-T. Liu, *Nanoscale* **2012**, *4*, 2272.
[21] L. Tingyi, P. Sen, K. Chang-Jin, *J. Microelectromech. Syst.* **2012**, *21*, 443.
[22] T. Daeneke, K. Khoshmanesh, N. Mahmood, I. A. de Castro, D. Esrafilzadeh, S. J. Barrow, M. D. Dickey, K. Kalantar-zadeh, *Chem. Soc. Rev.* **2018**, *47*, 4073.
[23] C. Karcher, V. Kocourek, D. Schulze presented at *Int. Scientific Colloquium, Modelling for Electromagnetic Processing*, Hanover, Germany March **2003**.

[24] S. Liu, K. Sweatman, S. McDonald, K. Nogita, *Materials* **2018**, *11*, 1384.
[25] D. S. Kim, H. Park, S. Y. Hong, J. Yun, G. Lee, J. H. Lee, L. Sun, G. Zi, J. S. Ha, *Appl. Surf. Sci.* **2019**, *471*, 300.
[26] S. Zhu, J.-H. So, R. Mays, S. Desai, W. R. Barnes, B. Pourdeyhimi, M. D. Dickey, *Adv. Funct. Mater.* **2013**, *23*, 2308.
[27] Y. R. Jeong, J. Kim, Z. Xie, Y. Xue, S. M. Won, G. Lee, S. W. Jin, S. Y. Hong, X. Feng, Y. Huang, J. A. Rogers, J. S. Ha, *NPG Asia Mater.* **2017**, *9*, e443.
[28] C. B. Cooper, K. Arutselvan, Y. Liu, D. Armstrong, Y. Lin, M. R. Khan, J. Genzer, M. D. Dickey, *Adv. Funct. Mater.* **2017**, *27*, 1605630.
[29] S.-Y. Tang, V. Sivan, P. Petersen, W. Zhang, P. D. Morrison, K. Kalantar-zadeh, A. Mitchell, K. Khoshmanesh, *Adv. Funct. Mater.* **2014**, *24*, 5851.
[30] S.-Y. Tang, K. Khoshmanesh, V. Sivan, P. Petersen, A. P. O'Mullane, D. Abbott, A. Mitchell, K. Kalantar-zadeh, *Proc. Natl. Acad. Sci. USA* **2014**, *111*, 3304.
[31] R. C. Gough, J. H. Dang, M. R. Moorefield, G. B. Zhang, L. H. Hihara, W. A. Shiroma, A. T. Ohta, *ACS Appl. Mater. Interfaces* **2016**, *8*, 6.
[32] C. B. Eaker, M. D. Dickey, *Appl. Phys. Rev.* **2016**, *3*, 031103.
[33] J. Wissman, M. D. Dickey, C. Majidi, *Adv. Sci.* **2017**, *4*, 1700169.
[34] J.-H. So, H.-J. Koo, M. D. Dickey, O. D. Velev, *Adv. Funct. Mater.* **2012**, *22*, 625.
[35] H.-J. Koo, J.-H. So, M. D. Dickey, O. D. Velev, *Adv. Mater.* **2011**, *23*, 3559.
[36] M. Wang, C. Trlica, M. R. Khan, M. D. Dickey, J. J. Adams, *J. Appl. Phys.* **2015**, *117*, 194901.
[37] G. J. Hayes, S. Ju-Hee, A. Qusba, M. D. Dickey, G. Lazzi, *IEEE Trans. Antennas Propag.* **2012**, *60*, 2151.
[38] M. R. Khan, C. B. Eaker, E. F. Bowden, M. D. Dickey, *Proc. Natl. Acad. Sci. USA* **2014**, *111*, 14047.
[39] X. Zhao, S. Xu, J. Liu, *Front. Energy* **2017**, *11*, 535.
[40] S.-Y. Tang, V. Sivan, K. Khoshmanesh, A. P. O'Mullane, X. Tang, B. Gol, N. Eshtiaghi, F. Lieder, P. Petersen, A. Mitchell, K. Kalantar-zadeh, *Nanoscale* **2013**, *5*, 5949.
[41] M. Pourbaix, *Atlas of Electrochemical Equilibria in Aqueous Solutions*, NACE International Cebelcor, Houston, TX **1974**.
[42] A. F. Stalder, T. Melchior, M. Müller, D. Sage, T. Blu, M. Unser, *Colloids Surf. A* **2010**, *364*, 72.
[43] V. Pulkki, M. Karjalainen, *Communication Acoustics: An Introduction to Speech, Audio and Psychoacoustics*, John Wiley & Sons, Hoboken, NJ **2015**.
[44] R. A. Serway, J. W. Jewett Jr., *Physics for Scientists and Engineers with Modern Physics*, 9th ed., Brooks/Cole, Boston, MA **2018**.
[45] M. R. Khan, C. Trlica, M. D. Dickey, *Adv. Funct. Mater.* **2015**, *25*, 671.
[46] H.-J. Koo, S. T. Chang, O. D. Velev, *Small* **2010**, *6*, 1393.
[47] M. F. Wang, M. J. Jin, X. J. Jin, S. G. Zuo, *Phys. Chem. Chem. Phys.* **2017**, *19*, 18505.
[48] N. H. Crowhurst, *Basic Audio*, Vol. *2*, John F. Rider Publisher, Inc., New York **1959**.
[49] A. Bokaian, *J. Sound Vib.* **1990**, *142*, 481.
[50] F. J. Fahy, P. Gardonio, *Sound and Structural Vibration: Radiation, Transmission and Response*, Academic press, Cambridge, MA **1985**.
[51] R.-H. M. Schmidt, Distortion Sources in Loudspeaker Drivers, https://www.rmsacoustics.nl/papers/whitepaperdistortion.pdf (accessed: September 2019).
[52] M. Kleiner, *Acoustics and Audio Technology*, 3rd ed., J. Ross Publishing, Fort Lauderdale, FL **2011**.

